

Wheat Oxophytodienoate Reductase Gene *TaOPR1* Confers Salinity Tolerance via Enhancement of Abscisic Acid Signaling and Reactive Oxygen Species Scavenging^{1[C][W]}

Wei Dong², Mengcheng Wang², Fei Xu, Taiyong Quan, Keqin Peng, Langtao Xiao, and Guangmin Xia*

Key Laboratory of Plant Cell Engineering and Germplasm Innovation, Ministry of Education, School of Life Science, Shandong University, Jinan, Shandong 250100, China (W.D., M.W., F.X., T.Q., G.X.); and Hunan Provincial Key Laboratory of Phytohormones and Growth Development, College of Bioscience and Biotechnology, Hunan Agricultural University, Changsha 410128, China (K.P., L.X.)

The 12-oxo-phytyldienoic acid reductases (OPRs) are classified into the two subgroups OPRI and OPRII. The latter proteins participate in jasmonic acid synthesis, while the function of the former ones is as yet unclear. We describe here the characterization of the OPRI gene *TaOPR1*, isolated from the salinity-tolerant bread wheat (*Triticum aestivum*) cultivar SR3. Salinity stress induced a higher level of *TaOPR1* expression in the seedling roots of cv SR3 than in its parental cultivar, JN177. This induction was abolished when abscisic acid (ABA) synthesis was inhibited. The overexpression of *TaOPR1* in wheat significantly enhanced the level of salinity tolerance, while its heterologous expression in *Arabidopsis* alleviated root growth restriction in the presence of salinity and oxidants and raised the sensitivity to ABA. In *Arabidopsis*, *TaOPR1* promoted ABA synthesis and the ABA-dependent stress-responsive pathway, partially rescued the sensitivity of the *Arabidopsis aba2* mutant defective in ABA synthesis to salinity, and improved the activities of reactive oxygen species scavengers and the transcription of their encoding genes while reducing malondialdehyde and reactive oxygen species levels. *TaOPR1* did not interact with jasmonate synthesis or the jasmonate signaling pathway. Rather than serving purely as an antioxidant, we believe that *TaOPR1* acts during episodes of abiotic stress response as a signaling compound associated with the regulation of the ABA-mediated signaling network.

Soil salinity represents an important constraint on plant growth and crop productivity, imposing a stress that encourages the production of reactive oxygen species (ROS). Plants have developed a complex ROS-scavenging system, the major components of which are a series of low- M_r nonenzymatic compounds such as ascorbate and glutathione and a set of enzymes including superoxide dismutase, catalase, and ascorbate peroxidase (Mittler, 2002). ROS-induced lipid peroxidation leads to the formation of a variety of cytotoxic molecules, some of which can be neutralized by members of the "Old Yellow Enzyme" (OYE) protein family, which is well represented in the yeast genome (Williams and

Bruce, 2002). The overexpression of *OYE2*, for example, lowers ROS levels and thereby protects the cell against apoptosis (Odat et al., 2007).

Plant 12-oxo-phytyldienoic acid reductases (OPRs) share some sequence similarity with OYE proteins and have been classified as FMN-dependent oxidoreductases. They are thought to catalyze the reduction of double bonds in α,β -unsaturated aldehydes and ketones. When presented with 12-oxo-phytyldienoic acid (OPDA) as a substrate, their activity generates 3-oxo-2(2'-pentenyl)-cyclopentane-1-octanoic acid (OPC-8:0; Schaller et al., 1998). Four isomers of OPDA have been described, namely cis-(+), cis-(-), trans-(+), and trans-(-) (Schaller et al., 1998). On the basis of their substrate specificity, the OPRs have split into two subgroups (Schaller and Weiler, 1997; Schaller et al., 1998, 2000; Strassner et al., 1999). Subgroup II members (OPRIIs; e.g. *AtOPR3*) can reduce all four OPDA isomers, but in planta their activity is largely focused on the reduction of cis-(+)-OPDA (Schaller et al., 1998). Since OPC8:0 is a precursor of jasmonic acid (JA), the OPRIIs are thought to be implicated in JA synthesis (Schaller et al., 1998). Subgroup I members (OPRIs; e.g. *AtOPR1* and *AtOPR2*), in contrast, are involved in the reduction of cis-(-)-OPDA (Strassner et al., 1999; Schaller et al., 2000), but their in vivo substrate(s) is unknown. It has been commonly suggested that the OPRI proteins are not enzymes in the octadecanoid pathway but rather serve some as yet unknown enzymatic function (Schaller et al., 1998). *OPRI* genes are typically up-regulated by pathogen invasion, wounding,

¹ This work was supported by the Natural Science Foundation of China (grant no. 31271303), the National Transgenic Project (grant no. 2011ZX08002-002), the National Basic Research 973 Program of China (grant nos. 2012CB114204 and 2009CB118300), and the Major Program of the Natural Science Foundation of China (grant nos. 31030053 and 91117006).

² These authors contributed equally to the article.

* Corresponding author; e-mail xiagm@sdu.edu.cn.

The author responsible for distribution of materials integral to the findings presented in this article in accordance with the policy described in the Instructions for Authors (www.plantphysiol.org) is: Guangmin Xia (xiagm@sdu.edu.cn).

[C] Some figures in this article are displayed in color online but in black and white in the print edition.

[W] The online version of this article contains Web-only data.
www.plantphysiol.org/cgi/doi/10.1104/pp.112.211854

and oxidative stress (Biesgen and Weiler, 1999; Strassner et al., 2002; Agrawal et al., 2003), events associated with ROS acceleration, so OPRI are claimed to be concerned with antioxidant activity (Fitzpatrick et al., 2003; Trotter et al., 2006; Beynon et al., 2009).

Notably, in addition to cis-(+)-OPDA, enzyme preparations from some plants, such as flax (*Linum usitatissimum*), may yield a substantial amount of the cis-(−) isomer (Laudert et al., 1997), and the latter may be an in vivo substrate for the OPRI. The allene oxide cyclase (AOC)-catalyzed enolization of 12,13-epoxyoctadecatrienoic acid to form OPDA generates a slow conversion of cis- to trans-isomer (Mueller and Brodschelm, 1994), and the generated trans-(+)-OPDA is also the substrate of OPRI (Schaller et al., 1998). Thus, the in vivo fate of OPR-mediated OPDA metabolism is likely to be much more diverse than simply the formation of JA. However, whether OPR activity is responsible for JA synthesis and signaling pathways is an open question. OPR genes are transiently regulated by wounding, low temperature, salinity, pathogen attack, and other environmental cues (Biesgen and Weiler, 1999; Strassner et al., 2002; Agrawal et al., 2003). In *Arabidopsis* (*Arabidopsis thaliana*), the OPRII gene *AtOPR3* is constitutively expressed throughout the plant, while the expression of the OPRI *AtOPR1* and *AtOPR2* is largely confined to the root (Biesgen and Weiler, 1999). It has been shown that plants are able to regulate the levels of OPDA and JA independently of one another (Parchmann et al., 1997; Stelmach et al., 1998), and evidence is accumulating that OPDA is a signaling compound in its own right (Weiler et al., 1994; Stelmach et al., 1998). OPR activity, therefore, may regulate the presence of its own substrates and thereby serve as an active regulatory component.

Bread wheat (*Triticum aestivum*) is one of the most important of our food crops, but it shows only limited tolerance to abiotic stress. Wheat 'SR3', with remarkable salinity tolerance, is bred from an asymmetric somatic hybrid between cv JN177 and tall wheatgrass (*Thinopyrum ponticum*; Xia et al., 2003; Xia, 2009). Transcriptomic and proteomic analyses have suggested that much of it can be ascribed to a superior level of ROS-scavenging capacity (Wang et al., 2008; Peng et al., 2009). Among the many genes differentially up-regulated by salinity stress in cv SR3 is one that encodes an OPR protein (Liu et al., 2012). Here, we show that this gene, denoted *TaOPR1*, responds to salinity stress in an abscisic acid (ABA)-dependent manner and that its overexpression in wheat and heterologous expression in *Arabidopsis* improve tolerance to salinity. This effect appears to operate through the regulation of ROS and ABA signaling pathways and is quite independent of JA synthesis and signaling.

RESULTS

TaOPR1 Transcription Was Induced by Various Stresses

The microarray analysis indicated that the level of *TaOPR1* transcription in cv SR3 plants was nearly 4-fold that in cv JN177 plants challenged with 200 mM

NaCl for 24 h, but the levels were identical after just 0.5 h (Fig. 1A). Real-time PCR analysis confirmed that *TaOPR1* transcript accumulated significantly over the course of 200 mM NaCl treatment and to a greater degree in cv SR3 than in cv JN177 after 24 and 48 h of treatment (Fig. 1B). High salinity often stimulates the production of ROS and ABA: the former causes severe oxidative damage, and the latter launches downstream stress-responsive pathways (Mittler et al., 2011). Here, the temporal transcription profiles of *TaOPR1* after exposure to 10 mM hydrogen peroxide (H₂O₂) and 100 μM ABA almost mirrored those under salinity stress in the two cultivars, and it also had stronger responsive patterns in cv SR3 than in cv JN177 (Fig. 1, C and D). Apart from ionic toxicity, high salinity also consists of osmotic stress (Munns and Tester, 2008). In the presence of 20% polyethylene glycol 6000 (PEG6000) to simulate osmotic stress, *TaOPR1* transcription rose markedly at an early stage, declining thereafter to a level that was still above the pretreatment one (Fig. 1E). These results demonstrate that *TaOPR1* is a stress-responsive gene, and its higher expression level in cv SR3 implies its positive role in stress tolerance. The accumulation of transcript induced by salinity stress was counteracted by the provision of norflurazon, an inhibitor of ABA synthesis (Fig. 1F), indicating that the gene's salinity-induced transcription was mediated by ABA.

TaOPR1 Is an OPR Gene Mapping to Wheat Chromosome 2B

The full-length *TaOPR1* complementary DNA (cDNA) comprises 1,347 bp, consisting of a 60-bp 5' untranslated region, a 1,110-bp open reading frame, and a 69-bp 3' untranslated region. The deduced peptide product comprises 369 residues and has an inferred molecular mass of 46 kD and a pI of 6.52. The phylogenetic analysis of the gene product indicated that *TaOPR1* belongs to the OPR subgroup and shares homology with rice (*Oryza sativa*) OPR6 (76%), maize (*Zea mays*) OPR4 (79%), and *Arabidopsis* OPR2 (67%; Fig. 2, A and B). The *TaOPR1* sequence retains the conserved residues that account for the NADPH- and FMN-binding sites of the OYE family (Fig. 2A). In order to know the chromosomal location of *TaOPR1*, aneuploid stocks of cv Chinese Spring were used as template for genomic PCR with *TaOPR1*-specific primers. The results showed that *TaOPR1* was not amplified from templates of stocks 2B2A, 2B2D, and D2BL, the former two of which lack the whole of chromosome 2B (2B is replaced by 2A and 2D, respectively) and the last of which lacks the short arm of 2B, while it was produced from the template of D2BS, which lacks the long arm of 2B (Fig. 2C). Thus, *TaOPR1* must map to the short arm of the second chromosome of the B genome (2BS). The location of the fluorescent signal produced by the transient expression of a *TaOPR1::GFP* fusion in *Arabidopsis* mesophyll protoplasts indicated that the cytoplasm is the site of *TaOPR1* deposition in planta (Fig. 2D). The cytoplasm location is due to the fact that *TaOPR1*, like

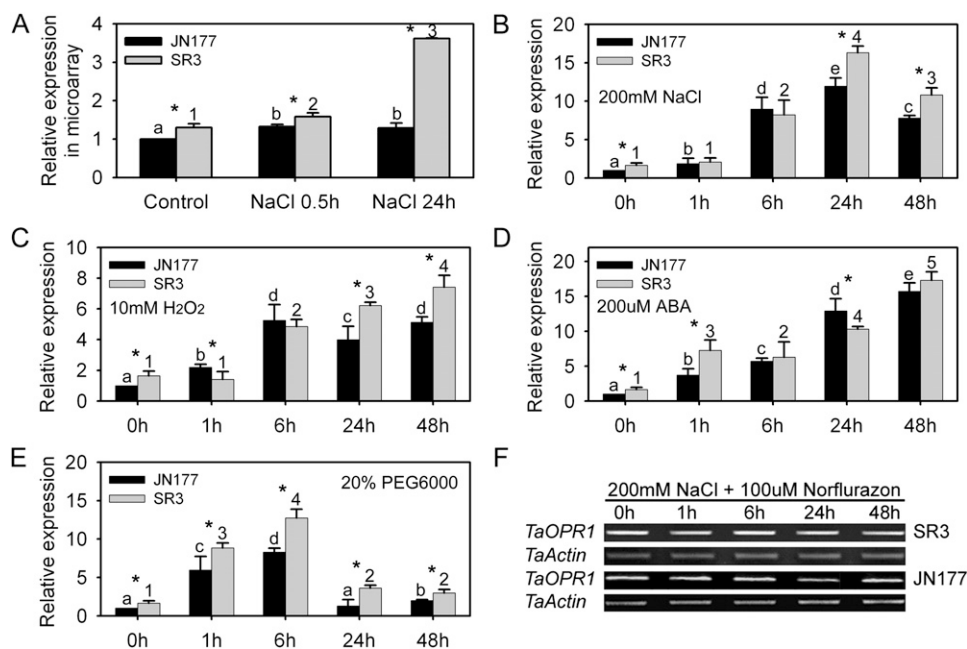


Figure 1. *TaOPR1* is induced by various abiotic stresses in wheat roots. A, cDNA microarray assay of *TaOPR1* transcription in cv SR3 and JN177 as affected by exposure to salinity stress. B to E, Real-time analysis of *TaOPR1* expression in cv SR3 and JN177 roots subjected to 200 mM NaCl (B), 200 μ M ABA (C), 10 mM H₂O₂ (D), and 20% (w/v) PEG6000 (E). F, Transcription of *TaOPR1* in cv SR3 and JN177 roots exposed to 200 mM NaCl and 100 μ M norflurazon (an inhibitor of ABA synthesis). Wheat seedlings at the three-leaf stage were used for analysis. Data are presented as means \pm sd. Bars marked with different letters (cv JN177) or numbers (cv SR3) indicate significantly different means using the one-way ANOVA LSD analysis ($P < 0.05$). The column at each time point marked with an asterisk indicates a significant difference between cv JN177 and SR3 using Student's *t* test analysis ($P < 0.05$).

other OPR1 proteins, lacks the OPR1-specific peroximal signal peptide at its C terminus (Fig. 2A), which is thought to determine the protein's localization to the peroxisome (Hayashi et al., 1996; Stintzi and Browse, 2000).

TaOPR1 Enhanced the Salinity Tolerance of Wheat and Arabidopsis

To ascertain whether the expression of *TaOPR1* has any effect on the level of salinity tolerance, it was transformed into both a highly sensitive wheat ('JN17') and into Arabidopsis ecotype Columbia (Col-0). Of the 12 independent transgenic overexpression (TaOE) lines of *TaOPR1* generated in wheat 'JN17', two (TaOE1 and TaOE2) were selected on the basis of the level of transgene expression (Fig. 3H). The two TaOE lines and the wild-type cv JN17 grew equally well in one-half-strength Hoagland liquid medium, and their seedling phenotype was indistinguishable (Fig. 3, A–C). However, after exposure to 200 mM NaCl, the wild-type seedlings became very wilted while the TaOE ones remained fully turgid (Fig. 3, D and E). The TaOE line shoots and roots were longer than those of the wild type (Fig. 3, E–G).

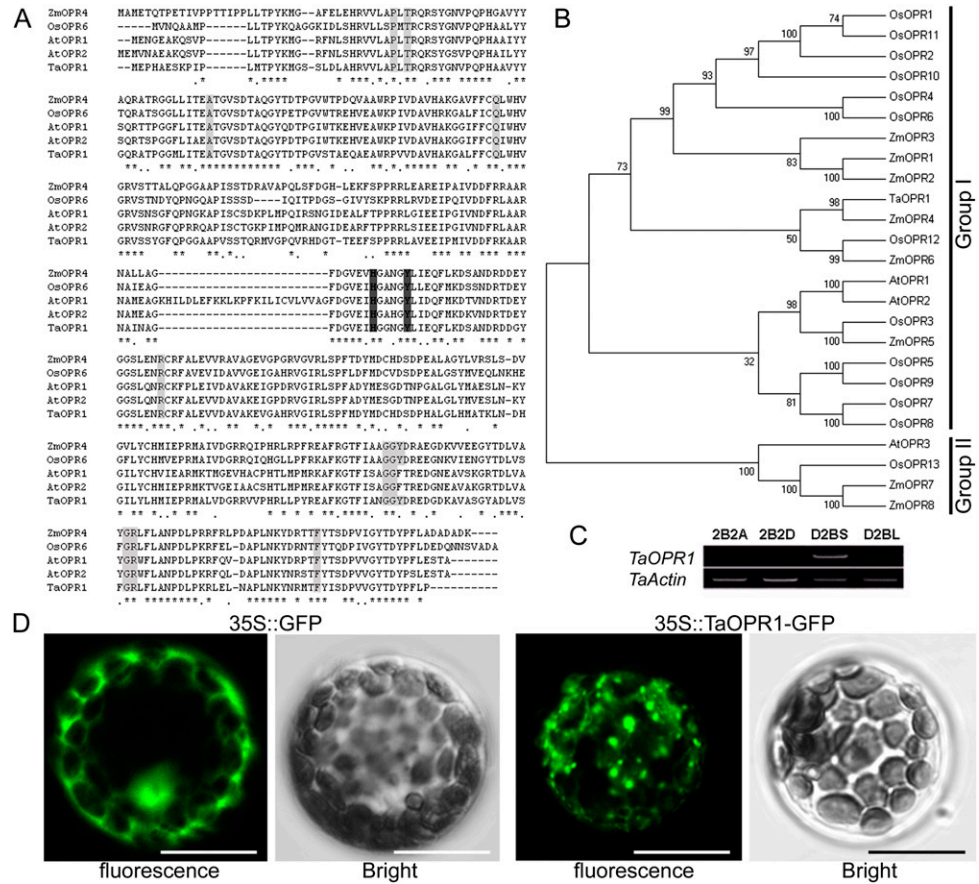
When the gene was heterologously expressed in Arabidopsis, there was no obvious phenotypic difference between the two highest expressors (AtOE1 and

AtOE2) and the empty vector control (VC), either when the plants were plated on Murashige and Skoog (MS) agar (Fig. 3, J and L) or when the seed was sown in soil (data not shown). However, in the presence of 100 or 125 mM NaCl, the Arabidopsis overexpressor (AtOE) lines were more vigorous than the VC line, forming larger leaves and longer primary roots (57% longer at 100 mM NaCl and 33% longer at 125 mM NaCl; Fig. 3, K and L). The germination rate also responded positively: in the absence of salinity, the AtOE and VC lines behaved indistinguishably, but in the presence of salinity, the AtOE lines were superior (Fig. 3M). Inconsistent with the positive effect of *TaOPR1*, the double RNA interference (RNAi) knockdown mutant *opr1opr2*, from two homologous OPR1 genes in Arabidopsis (Beynon et al., 2009), did not increase the sensitivity to NaCl treatment, and their phenotypes were comparable to the wild type (Supplemental Fig. S1, A and C).

TaOPR1 Reduced the Sensitivity to H₂O₂ in Arabidopsis

Tolerance to salinity stress has frequently been associated with tolerance to oxidative stress. Specifically, *TaOPR1* overexpressor lines exhibited superior growth status in comparison with the VC line in the presence of 1.0 and 1.5 mM H₂O₂; after 10 d of exposure to H₂O₂, the primary roots of overexpressor lines were significantly

Figure 2. *TaOPR1* encodes an OPR1 protein that locates in the cytoplasm. A, Peptide alignment of *TaOPR1* and other OPR subgroup I members. Residues shown in black or gray are conserved. B, Phylogenetic analysis indicates that *TaOPR1* is a subgroup I member. C, Aneuploid analysis shows that *TaOPR1* maps to the short arm of wheat chromosome 2B. 2B2A and 2B2D are wheat nullitetrasonic lines whose chromosome 2 of the B genome (2B) is replaced by chromosome 2 of the A (2A) and D (2D) genomes, respectively; D2BS and D2BL are wheat ditelocentric lines that lack the long arm and short arm of chromosome 2B, respectively. D, *TaOPR1* is deposited in the cytoplasm, as indicated by the fluorescent signal generated from a transiently expressed *TaOPR1::GFP* fusion protein in the Arabidopsis protoplast. The control experiment employed a simple *GFP* transgene. Bars = 10 μ m. [See online article for color version of this figure.]



longer than those of the VC line (Fig. 4, A and B), indicating that *TaOPR1* overexpression reduced sensitivity to H₂O₂. Additionally, similar results were also obtained when the plants were supplied with higher levels (2, 3, and 5 mM) of H₂O₂ for 3 weeks (data not shown). Unlike *TaOPR1*-overexpressing lines, the sensitivity to H₂O₂ was not altered in Arabidopsis *opr1opr2* mutants (Supplemental Fig. S1, A and B).

The tolerance to oxidative stress closely links to the homeostasis between ROS scavenging and production, so we further measured the transcription of some ROS scavengers and producers as well as the activities of their products. In the absence of stress, the activities of peroxidase (POD) and catalase (CAT) in the AtOE lines were 20% and 40%, respectively, above that in the VC line (Fig. 4C), and these two ROS-scavenging enzymes were similarly more active in the TaOE lines than in the wild type (Fig. 4E). The content of malondialdehyde (MDA), an indicator of intracellular ROS damage, in the AtOE seedlings was 20% less than in the VC ones (Fig. 4D). The real-time PCR analysis confirmed that the transcription of *AtCAT1*, *AtCAT2*, *AtAPX1* (for ascorbate peroxidase1), and *AtAPX2* was about 5-, 2-, 1.5-, and 5-fold higher, respectively, in the AtOE lines than in VC (Fig. 4F). The gene encoding *AtZAT10*, a protein that enhances the expression of *AtAPX2* (Mittler et al., 2006), was also up-regulated (Fig. 4F). The transcription of *AtSOD* and *AtGPX*, encoding

superoxidase dismutase and glutathione peroxidase, respectively, behaved similarly between AtOE and VC lines (Supplemental Fig. S2A). ROS is majorly produced by the catalysis of NADPH oxidase. *AtRBOHC*, *AtRBOHD*, and *AtRBOHF*, encoding three subunits of NADPH oxidase, were unaffected by the presence of *TaOPR1* (Supplemental Fig. S2A). The ROS levels of the overexpressor and VC lines were visualized by 3,3'-diaminobenzidine (DAB) staining, and the staining signals in 3-week-old seedlings of two overexpressor lines were distinguishably weaker than those in the VC line (Fig. 4G). These results demonstrate that *TaOPR1* can reduce intracellular levels of ROS by promoting the capacity of its removal.

TaOPR1 Heightened ABA Sensitivity in Arabidopsis

The AtOE lines were highly sensitive to the provision of exogenous ABA. In the absence of exogenous ABA, the germination rate of the AtOE and VC lines was indistinguishable; however, in the presence of 0.25 μ M ABA, the germination rate of the AtOE lines was only 40% after 1 d and reached 90% after 3 d, whereas for both VC and wild-type Col-0, the equivalent proportions were nearly 80% and almost 100% (Fig. 5A). The effect of the higher levels of ABA (0.5 and 0.75 μ M) was to suppress the germination over the first 4 d of the AtOE lines more severely than in either the VC or the wild-type line (Fig. 5A). By the second day, approximately

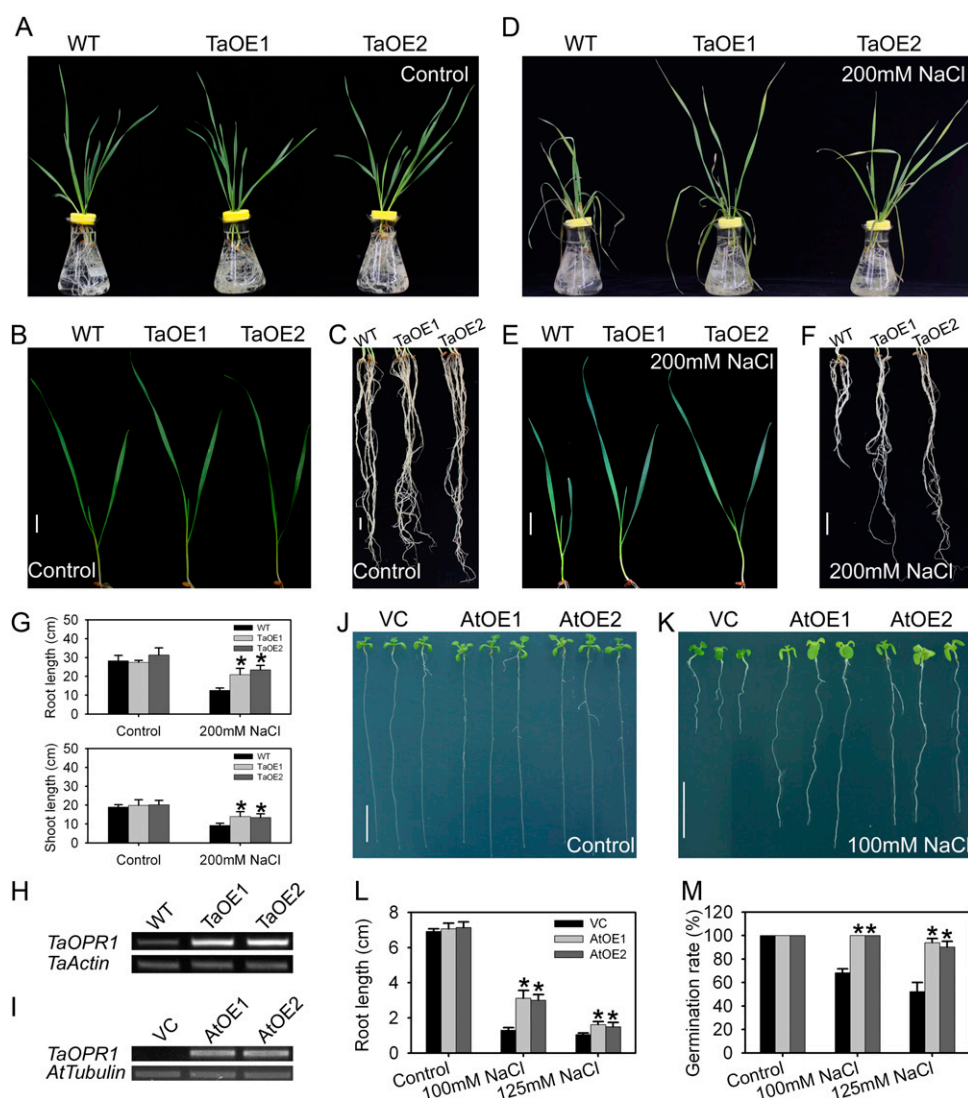


Figure 3. *TaOPR1* contributes to the salinity tolerance of wheat and Arabidopsis. A to F, Seedling phenotypes of wild-type (WT) wheat (the salinity-sensitive cultivar JN17) and *TaOE1* and *TaOE2* (transgenic wheat lines overexpressing *TaOPR1*) in response to 200 mM NaCl for 4 d. The treatment involved a pretreatment of the daily addition of 50 mM NaCl up to 200 mM. G, Root and shoot lengths of salinity-stressed wheat seedlings. H and I, RT-PCR analysis indicated that the *TaOPR1* transgene was successfully transcribed in both wheat and Arabidopsis. Wheat *Actin* and Arabidopsis *Tubulin* genes were used as internal references. J and K, Arabidopsis seedling response to a 12-d exposure to salinity stress. *AtOE1* and *AtOE2*, Transgenic lines heterologously expressing *TaOPR1*; VC, transgenic line carrying an empty pSTART vector. L, Root length of salinity-stressed Arabidopsis seedlings. M, Germination rate of Arabidopsis. Data are presented as means \pm SD, and columns marked with asterisks indicate significant differences from the VC line under the control or in each treatment using Student's *t* test analysis ($P < 0.05$). Bars = 1 cm.

60% of Col-0 and VC seeds had germinated in the presence 0.5 μ M ABA and approximately 25% had germinated in the presence of 0.75 μ M ABA; at the same time point, respectively, just approximately 20% and approximately 10% of the *AtOE* seed had germinated. The germination rates of Col-0, VC, and *AtOE* all achieved approximately 100% germination by 5 d (Fig. 5A). The proportion of *AtOE* seedlings bearing green cotyledons was markedly lower than in VC and Col-0 seedlings (Fig. 5A). Under nonstressed conditions, both the leaf and root growth of the *AtOE* lines were similar to those of the VC line. In the presence of 2 μ M ABA, in comparison with the VC line, root growth in the *AtOE* lines was reduced by approximately 24%, and higher concentrations (5 and 10 μ M) reduced it by more than 30% (Fig. 5, B and C).

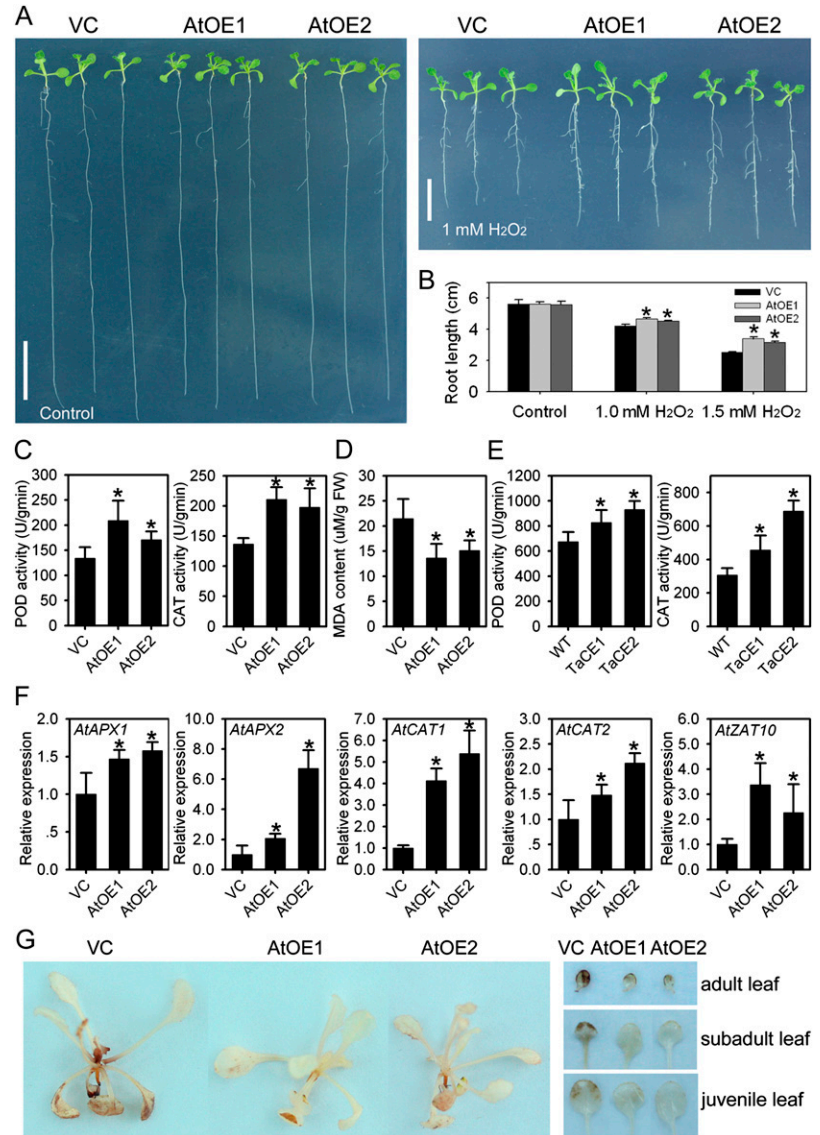
TaOPR1 Stimulated the ABA-Dependent Stress-Responsive Pathway

When the expression levels of a set of well-known stress response genes were monitored, *AtRD22*, *AtRD29A*, and

AtRD29B proved to have been substantially up-regulated in the *AtOE* lines, as were the two upstream transcription factors *AtMYB2* and *AtMYC2* (Fig. 6, B and C). Since these genes are all key components of the ABA-dependent stress-responsive signaling pathway in Arabidopsis, the transcript abundance of *AtNCED3* and *AtAAC3* was monitored and shown to be up-regulated as well (Fig. 6A). In contrast, among stress-responsive genes acting independently of ABA, all known components had no obviously differential expression in the *AtOE* lines (Supplemental Fig. S2, B and C).

To further confirm the role of ABA in *TaOPR1*-enhanced salinity stress, *TaOPR1* was transformed into the Arabidopsis *aba2* mutant, which is defective in ABA synthesis, to construct *TaOPR1/aba2* lines. *TaOPR1/aba2*, *aba2*, and VC seedlings appeared comparable with each other under nonstress conditions (Fig. 6D). Salinity stress seriously restricted the growth of *aba2* seedlings, and in comparison with the VC line, the leaves were much smaller and root lengths were shorter by more than 50% under two levels of NaCl treatment (Fig. 6, E

Figure 4. *TaOPR1* confers H₂O₂ tolerance by promoting ROS-scavenging capacity. A, Phenotypes of seedlings exposed to H₂O₂ for 10 d. AtOE1 and AtOE2, Transgenic lines heterologously expressing *TaOPR1*; VC, transgenic line carrying an empty pSTART vector. B, Root length of Arabidopsis. C, POD and CAT activities of Arabidopsis. D, MDA content of Arabidopsis. E, POD and CAT activities of wheat. WT, Wild type. F, Relative transcription levels of genes encoding ROS-scavenging enzymes in Arabidopsis (real-time PCR data). G, ROS levels of Arabidopsis by DAB staining. For C, D, F, and G, 2-week-old Arabidopsis seedlings cultured on medium plates were used; for E, three-leaf-stage wheat seedling leaves harvested from plants raised in one-half-strength Hoagland liquid medium were sampled. Data are presented as means \pm SD, and columns marked with asterisks indicate significant differences from the VC line under the control or in each treatment using Student's *t* test analysis ($P < 0.05$). Bars = 1 cm. [See online article for color version of this figure.]



and G). *TaOPR1* overexpression obviously rescued the phenotype of *aba2* when challenged with NaCl treatments: the root lengths of *TaOPR1/aba2* lines were about 70% and 60% of those of the VC line, and the leaf sizes between *TaOPR1/aba2* and VC lines had no significant difference (Fig. 6, E and G). However, *TaOPR1* did not alleviate the sensitivity of *aba2* to H₂O₂: the root lengths of *TaOPR1/aba2* and *aba2* seedlings were similar, which was significantly shorter than the VC line (Fig. 6, F and H).

TaOPR1 Did Not Disturb JA Synthesis and Signaling

The effect of heterologous *TaOPR1* expression on the response to exogenously supplied JA and on JA synthesis and signaling genes was then investigated. The growth of both the AtOE and VC root and leaf was restricted by the presence of either 3 or 5 μ M JA (Fig. 7A). Among genes encoding enzymes involved in JA synthesis, *AtAOC1* was clearly up-regulated in the

AtOE lines, but *AtAOC2*, *AtAOC3*, and *AtAOC4* were not differentially transcribed; *AtOPR3* expression was not influenced by the heterologous expression of *TaOPR1* (Fig. 7B). Following the transcription of JA synthesis genes, JA levels of AtOE lines were not altered in comparison with the VC line (Fig. 7C). Moreover, no transcriptional difference was found in either *AtCO11* or *AtJAZ1* (both of which are components of the JA signaling pathway; Fig. 7B). Within two OPR1 genes, *AtOPR1* but not *AtOPR2* was reduced in the AtOE lines (Fig. 7B).

DISCUSSION

TaOPR1 Confers Salinity Tolerance by Enhancing Antioxidation Capacity

Salinity stress is associated with the production of ROS, so a component of tolerance is represented by the plant's ability to cope with higher levels of these

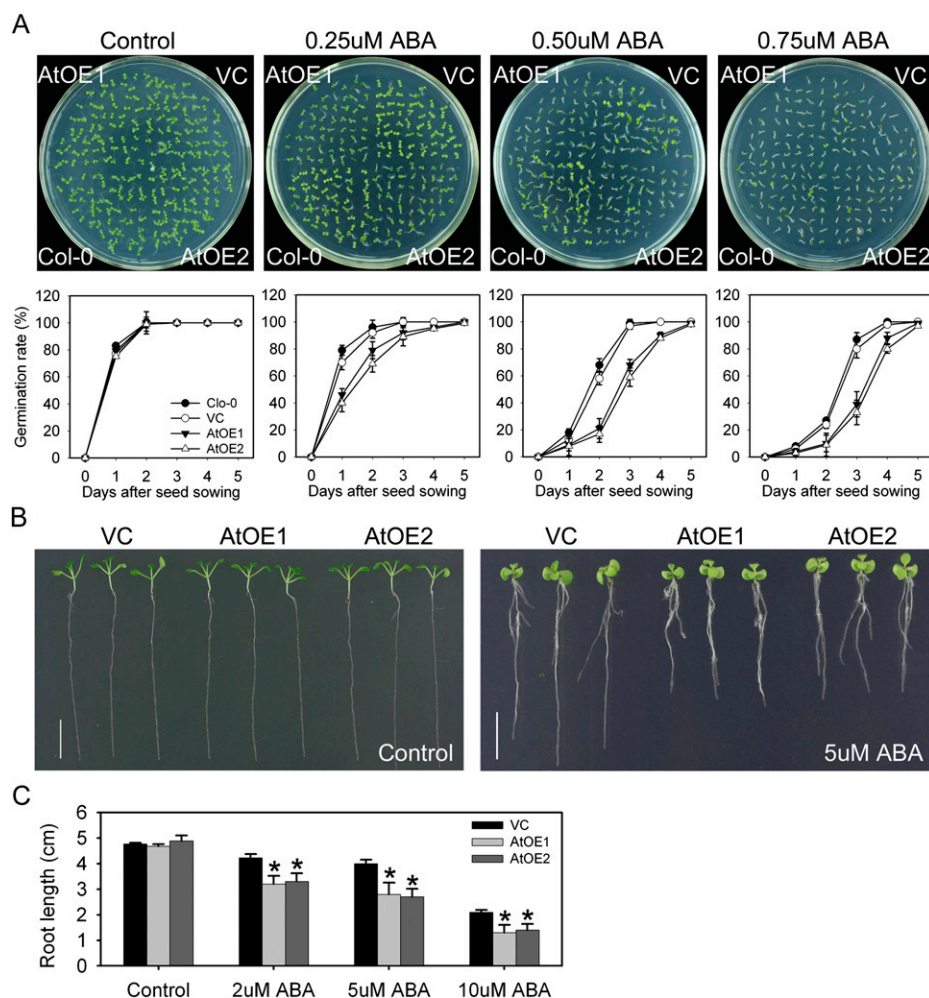


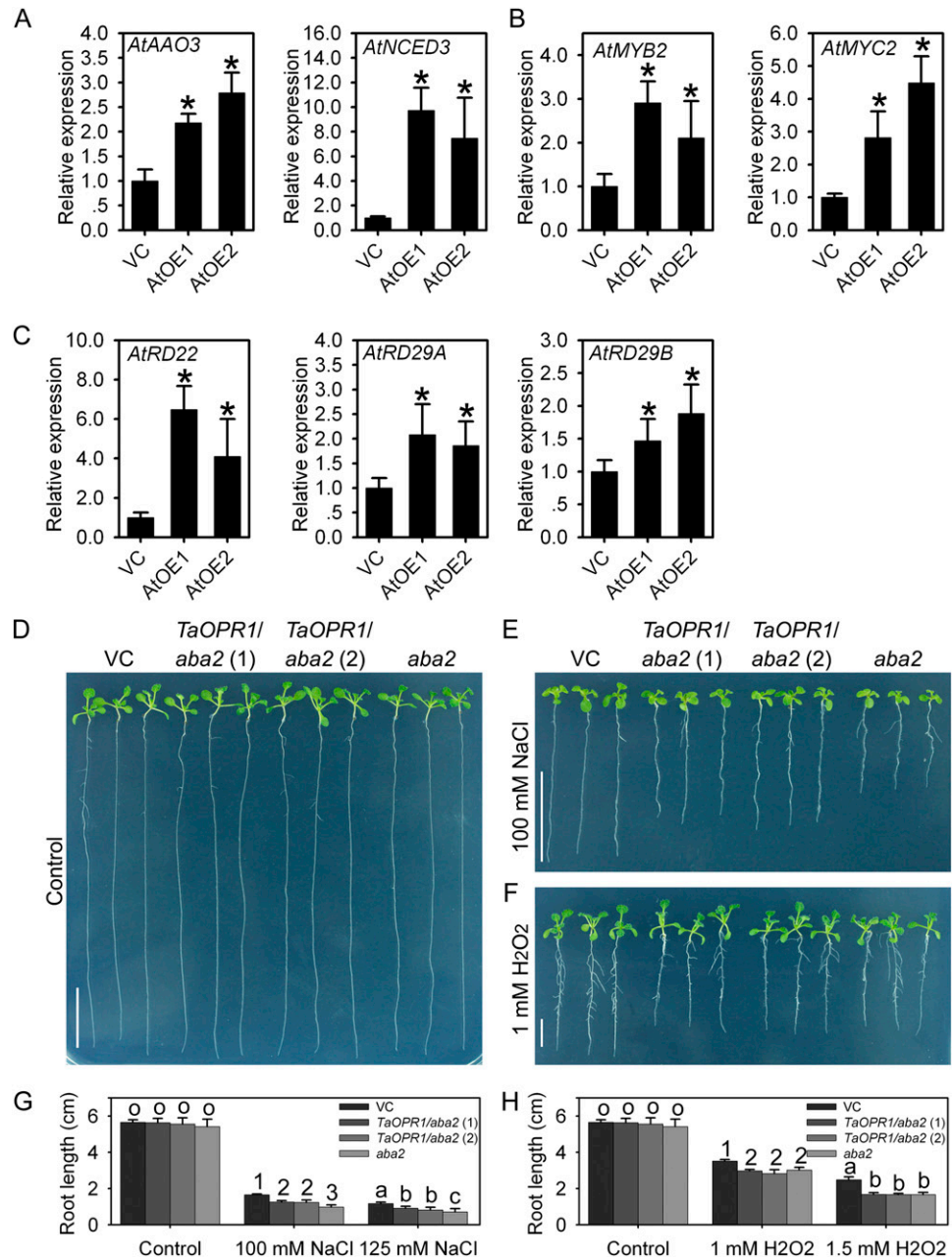
Figure 5. *TaOPR1* increases the ABA sensitivity of Arabidopsis. A, Delayed germination in the presence of ABA treatment. AtOE1 and AtOE2, Transgenic lines heterologously expressing *TaOPR1*; VC, transgenic line carrying an empty pSTART vector. B, *TaOPR1* suppresses the growth of seedlings exposed to ABA for 10 d. C, Root lengths of seedlings shown in B. Data are presented as means \pm SD, and columns marked with asterisks indicate significant differences from the VC line under the control or in each treatment using Student's *t* test analysis ($P < 0.05$). [See online article for color version of this figure.]

harmful molecules. Excess ROS in the cell causes extensive lipid peroxidation, which generates a range of toxic breakdown products, such as the α,β -unsaturated aldehydes (Esterbauer, 1993; Trotter et al., 2006). The antioxidation property of the OPRs is thought to operate via the reduction of double bonds in these products (Esterbauer, 1993; Trotter et al., 2006). For example, AtOPR1 can efficiently reduce the double bond of trinitrotoluene to form reduced trinitrotoluene derivatives, both in vitro and in vivo (Beynon et al., 2009). The reactive aldehyde MDA has been identified to reflect the extent of ROS-induced lipid peroxidation (Nankivell et al., 1994), so the decrease in MDA contents in AtOE lines (Fig. 4D) indicates that *TaOPR1* certainly alleviates ROS damage. However, *TaOPR1* overexpression in the *aba2* genetic background did not reduce the sensitivity to H_2O_2 (Fig. 6, F and H), suggesting that the role of *TaOPR1* in ROS damage alleviation is not achieved through its direct reduction ability on the reactive products of lipid peroxidation.

In addition to counteracting the toxicity of ROS-induced lipid peroxidation, the direct neutralization of ROS has been proposed as a component of stress tolerance (Mittler, 2002). The OYZ family is believed to

protect the cell against the damaging effects of lipid peroxidation products, and the function of OYE in yeast also appears to be to reduce the level of ROS present (Fitzpatrick et al., 2003). However, yeast strains deficient for *OYE2* are hypersensitive to acrolein, a ubiquitous reactive aldehyde formed from lipid peroxidation, but show little sensitivity to exogenous H_2O_2 (Trotter et al., 2006). This demonstrates a diverse role for OYE family proteins in the response to direct oxidative stress. Here, *TaOPR1* overexpression elevated the activities of several ROS-scavenging enzymes and the transcription of their encoding genes (Fig. 4, C–F). *AtZAT10*, which has been shown to promote the transcription of *AtAPX2* (Mittler et al., 2006), was also up-regulated in the AtOE lines (Fig. 4F). Thus, there is some evidence that *TaOPR1* promotes the efficiency of ROS scavenging to affect ROS removal rather than protects cells from ROS-induced lipid peroxidation. ABA enhances the transcription and activity of ROS network genes, and defects in this network can also disrupt the expression of ABA and stress-responsive genes (Miao et al., 2006). Along with the fact that *TaOPR1/aba2* did not rescue the sensitivity of *aba2* to H_2O_2 (Fig. 6, F and H), it could be concluded that the enhancement of ROS scavenging promoted by *TaOPR1*

Figure 6. *TaOPR1* accounts for salinity tolerance by promoting the ABA signaling pathway and decreases H₂O₂ sensitivity in an ABA-dependent manner. A to C, Relative transcription levels in 2-week-old seedlings of genes involved in ABA synthesis and the ABA-dependent stress response pathway (real-time PCR data). D to F, Phenotypes after exposure to exogenous NaCl for 12 d and to H₂O₂ for 10 d. *TaOPR1/aba2* (1) and *TaOPR1/aba2* (2), *aba2* mutant lines heterologously expressing *TaOPR1*; VC, transgenic line carrying an empty pSTART vector. G and H, Root lengths of seedlings shown in D to F. Data are presented as means ± SD. In A to C, columns marked with asterisks indicate significant differences from the VC line using Student's *t* test analysis (*P* < 0.05); in G and H, bars in each column marked with different letters or numbers indicate significantly different means using the one-way ANOVA LSD analysis (*P* < 0.05). [See online article for color version of this figure.]



expression may be, at least in part, mediated by an acceleration of ABA synthesis and an up-regulation of relevant signaling pathways.

The Interplay between *TaOPR1* and the ABA-Mediated Salinity-Responsive Pathway

ABA is a vital component of the abiotic stress response, and a boost in ABA synthesis and/or a limitation to its degradation is a frequently observed plant response to abiotic stress (Jakab et al., 2005). ABA is often recruited as the primary signal activating the transcription of stress-responsive genes (Lee and Luan, 2012).

TaOPR1 is induced by both salinity and ABA, while ABA synthesis inhibition largely counteracted the salinity-induced accumulation of *TaOPR1* transcript (Fig. 1, B and C). Therefore, there is a reasonably strong case that the induction of *TaOPR1* expression operates via an increase in the rate of ABA synthesis. ABA triggers a signaling cascade that up-regulates a suite of abiotic stress-responsive genes (Nakashima et al., 2009). The Arabidopsis genes *AtRD22*, *AtRD29A*, and *AtRD29B* are all up-regulated via an ABA-dependent pathway (Fujita et al., 2011). *AtRD22* is known to be regulated by the transcription factors *AtMYB2* and *AtMYC2* (Abe et al., 2003). The enhancement of ABA sensitivity (Fig. 5), mirroring the effect of *AtMYB2* and *AtMYC2* overexpression

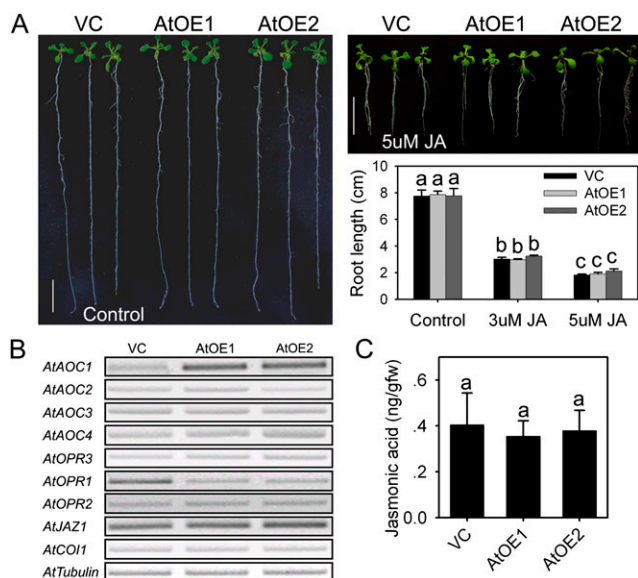


Figure 7. *TaOPR1* in Arabidopsis influences neither JA synthesis nor the JA signaling pathway. A, Seedling phenotypes and root length comparison following JA treatment for 16 d. AtOE1 and AtOE2, Transgenic lines heterologously expressing *TaOPR1*; VC, transgenic line carrying an empty pSTART vector. B, Transcription of genes involved in JA synthesis and signaling pathways in 2-week-old seedlings (RT-PCR data). C, JA levels (ng g^{-1} fresh weight) of 2-week-old seedlings detecting by LC-MS/MS. Data are presented as means \pm SD, and bars marked with different letters indicate significantly different means using the one-way ANOVA LSD analysis ($P < 0.05$). [See online article for color version of this figure.]

(Abe et al., 2003), and the transcription elevation of these genes in AtOE lines (Fig. 6, B and C) provide firm evidence for a positive role of *TaOPR1* in stress-responsive ABA signaling.

TaOPR1 expression also markedly increased the transcript abundance of *AtNCED3* and *AtAAO3* (Fig. 6A), which encode proteins responsible for the catalysis of two key steps in the ABA synthesis pathway. The suggestion is that an acceleration in the ABA-dependent pathway caused by *TaOPR1* expression is initiated from a burst in ABA synthesis. Given the partially rescued phenotype of *aba2* under salinity stress (Fig. 6, E and G), it is reasonable to claim that *TaOPR1* regulates ABA synthesis and ABA signaling pathways separately. Thus, we speculate that, in addition to the well-documented cross talk between OPRII-generated JA and ABA (Kazan and Manners, 2011), OPRIs can also interact with ABA-mediated pathways.

TaOPR1 Does Not Disturb JA Synthesis and Signaling Machinery

Although the in planta OPRi substrates have yet to be identified, they are known to be able to reduce, to a moderate extent at least, trans-(+)-OPDA, a stereoisomer converted from cis-(+)-OPDA, the intermediate precursor of JA (Mueller and Brodschelm, 1994). The

AOCs catalyze the formation of cis-(+)-OPDA from 12,13-epoxyoctadecatrienoic acid, a reaction regarded as important in both octadecanoid and JA synthesis (Mueller and Brodschelm, 1994). Of the four AOC genes present in Arabidopsis, *AtAOC2* is the most effective in the formation of cis-(+)-OPDA, and this copy also shows the strongest response to wounding (Stenzel et al., 2003). Neither the transcript of JA synthesis genes nor the level of endogenous JA was dependent on *TaOPR1* expression (Fig. 7, B and C). These observations indicate that JA synthesis is out of *TaOPR1*, a conclusion supported by the lack of any differential transcription of the JA receptor gene *AtCOI1* or of *JAZ1* (Fig. 7B). *AtMYC2* is activated by JA, which allows it to be a pivotal mediator in both the ABA and JA signaling pathways (Katsir et al., 2008; Yan et al., 2009). The behavior of the AtOE lines allows the conclusion to be drawn that the induction of *AtMYC2* was due to a promotion of the ABA but not of the JA signaling pathway and, hence, that *TaOPR1* exerts no regulatory activity over the JA synthesis and signaling machinery.

AtAOC1 was induced in the AtOE lines (Fig. 7B), which appears inconsistent with the lack of interaction with JA synthesis and the JA signaling pathway. The distinct functions of the various AOCs are not as yet well defined, because no clear correlation has been established between their transcription and the synthesis of JA (Kramell et al., 2000; Miersch and Wasternack, 2000; Ziegler et al., 2001; Stenzel et al., 2003; Delker et al., 2006). A possible scenario is that the enolization that allows the slow conversion of cis- to trans-OPDA isomers is catalyzed by *AtAOC1*. If the heterologous expression of *TaOPR1* utilizes more trans-(+)-OPDA, this could provide a positive feedback loop to promote the expression of *AtAOC1*. AOCs are known to differ

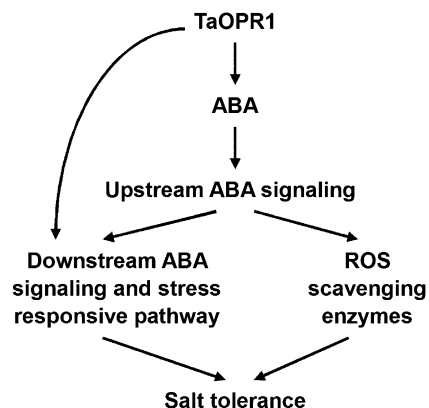


Figure 8. Hypothetical model of *TaOPR1* action in Arabidopsis. *TaOPR1* promotes ABA synthesis and signaling pathways, which elevates the activity occurring within the ABA-dependent abiotic stress-responsive pathway and increases the level of ROS-scavenging activity, thereby accounting for salinity tolerance. *TaOPR1* can also directly improve downstream ABA signaling and the ABA-dependent stress-responsive pathway in an ABA synthesis-independent manner.

in their substrate specificity, either arising from α -linolenic acid and leading to the synthesis of OPDA or from hexadecatrienoic acid and leading to the synthesis of dinor-OPDA (Weber et al., 1997; Reymond et al., 2000; Stenzel et al., 2003; Delker et al., 2006). Whether the OPRIs, along with AOC1, participate in the synthesis and/or metabolism of other lipid fatty acid derivatives is a question that deserves some attention.

The AtOE lines accumulated less *AtOPR1* transcript than the VC line, while the transcript abundance of *AtOPR2* was independent of *TaOPR1* expression (Fig. 7B). *AtOPR1* is up-regulated during leaf senescence by some 2-fold, but *AtOPR2* appears to be constitutively expressed during the course of leaf development (He et al., 2002). Thus, although these two OPR1 gene sequences are highly similar to one another and are both predominantly expressed in the root (Biesgen and Weiler, 1999), their regulation, if not their function as well, appears to have diverged. The repression of *AtOPR1* by the *TaOPR1* transgene suggests a negative feedback regulatory effect, perhaps based on functional redundancy between *TaOPR1* and *AtOPR1*.

Our overall proposition is that *TaOPR1* expression is induced by a boost in ABA synthesis prompted by abiotic stress and that this, in turn, promotes ABA synthesis. *TaOPR1* promotes ABA synthesis and signaling pathways, which elevates the level of activity within the ABA-dependent abiotic stress-responsive signaling pathway and increases the level of ROS-scavenging activity, thereby explaining the positive effect of *TaOPR1* on the salinity (and other abiotic stress) tolerance of Arabidopsis; besides, *TaOPR1* can also accelerate the ABA-dependent abiotic stress-responsive signaling pathway in ABA synthesis-independent behavior (Fig. 8). The function of *TaOPR1* may lie in the metabolism of trans-(+)-OPDA, with consequent effects on the workings of the (ABA-dependent-responsive and/or ROS) signaling pathway that this molecule mediates. At the same time, since the slow conversion to trans-(+)-OPDA would likely not sufficiently alter the size of the cis-(+)-OPDA pool, the presence of *TaOPR1* does not induce any change in JA synthesis or in the JA signaling pathway. We have assembled a body of evidence to show that the products of various OPDA isomers catalyzed by the two OPR subgroups can cross talk with ABA, while there is little sign of any interplay within the two subgroups. How *TaOPR1* performs these roles, especially whether *TaOPR1* operates via the catalysis of trans-(+)-OPDA, has yet to be elucidated.

MATERIALS AND METHODS

Isolation of the *TaOPR1* Full-Length cDNA and Characterization of Its Sequence

The fragment of the OPR1 homolog identified via microarray analysis was used as a BLASTN query against the wheat (*Triticum aestivum*) EST database held at the National Center for Biotechnology Information. All matching ESTs were assembled using CAP3 software, and a pair of gene-specific primers designed from this assembly (Supplemental Table S1) was used to amplify a

full-length cDNA from a cv SR3 cDNA library. The PCR consisted of a 3-min denaturation at 94°C, followed by 35 cycles of 94°C/30 s, 59°C/30 s, and 72°C/90 s, with a final extension of 72°C/5 min. The amplicon was inserted into the pMD18-T vector (Takara), following the supplier's instructions, and submitted for sequencing. The sequence, designated *TaOPR1*, was used to construct a phylogeny using a neighbor-joining method implemented within ClustalX and MEGA5 software (Kumar et al., 2004; Larkin et al., 2007), and its predicted peptide product *TaOPR1* was aligned with other OPRIs using ClustalX software (Larkin et al., 2007).

Plant Materials and Treatments

Seedlings of cv SR3 and of its parental wheat cultivar JN177 were raised to the three-leaf stage in one-half-strength Hoagland liquid medium under a 16-h photoperiod at 22°C, after which they were transferred for up to 48 h to the same medium containing 200 mM NaCl, 20% (w/v) PEG6000, 10 mM H₂O₂, 100 mM ABA, or 100 mM ABA/100 mM norflurazon/200 mM NaCl. A *pCam23A::TaOPR1* construct driven by the ubiquitin promoter was introduced into the salinity-sensitive wheat 'JN17' using the shoot apical meristem method described by Zhao et al. (2006). Ten-day-old seedlings of both transgenic and wild-type plants were raised in one-half-strength Hoagland liquid medium with or without NaCl under a 16-h photoperiod at 22°C. The NaCl treatment involved the daily addition of 50 mM NaCl until the concentration had reached 200 mM. The seedlings were held in this solution for a further 4 d. All measurements were carried out with three repeats.

Transgenic forms of Arabidopsis (*Arabidopsis thaliana*) Col-0 were made by introducing a *pSTART::TaOPR1* construct driven by the cauliflower mosaic virus 35S promoter (or just an empty vector) using the floral dip method (Clough and Bent, 1998). Surface-sterilized seeds were plated on one-half-strength MS agar medium, kept in the dark at 4°C for 2 d to break dormancy, and subsequently transferred to a 16-h photoperiod at 22°C for 2 d. They were then replated on one-half-strength MS agar medium supplemented with 0, 100, or 125 mM NaCl for 12 d, with 0, 1.0, or 1.5 mM H₂O₂ for 10 d, with 0, 2, 5, or 10 μ M ABA for 10 d, or with 0, 3, or 5 μ M JA for 16 d and held under a 16-h photoperiod at 22°C. A germination assay was conducted by plating surface-sterilized seeds on one-half-strength MS agar medium containing 0, 125, or 175 mM NaCl as well as 0, 0.25, 0.5, or 0.75 μ M ABA. After holding for 48 h at 4°C in the dark, the plates were transferred to a 16-h photoperiod at 22°C for 5 d. The emergence of the radicle was taken as representing a successfully germinated seed. Germination rates were expressed as the proportion of seeds that had successfully germinated. The experiment was replicated three times.

Reverse Transcription-PCR and Real-Time PCR Analyses

Total RNA was extracted from both wheat roots and Arabidopsis seedlings using the Trizol Reagent (Invitrogen) and treated with DNase I. The first cDNA strand synthesized using a Moloney murine leukemia virus reverse transcription (RT) system kit (Invitrogen) according to the manufacturer's instructions was used as the template for 20- μ L RT-PCRs containing 1 \times Easy Taq buffer (Transgene), 1 unit of EasyTaq (Transgene), 100 μ M deoxyribonucleotide triphosphates, 0.5 μ M forward and 0.5 μ M reverse primers (sequences given in Supplemental Table S1), and 1 μ L of a 1:10 dilution of the cDNA. The PCR regime consisted of a 5-min denaturation at 94°C, followed by 28 cycles of 94°C/30 s, 55°C/30 s, and 72°C/30 s, completed by an extension step of 10 min at 72°C. The 20- μ L real-time PCRs contained 10 μ L of 2 \times SYBR Premix Ex Taq mix (Takara), 0.2 μ M forward and 0.2 μ M reverse primers (sequences given in Supplemental Table S1), and 1 μ L of a 1:10 dilution of the cDNA first strand, and the cycling regime was composed of a denaturation step of 95°C/2 min, followed by 45 cycles of 95°C/10 s, 60°C/20 s, and 72°C/20 s. A melting-curve analysis was performed over the range 80°C to 95°C at 0.5°C intervals. Relative gene expression levels were detected using the comparative threshold cycle method 2^{- $\Delta\Delta$ CT} (Livak and Schmittgen, 2001). A positive control was provided by a parallel analysis based on a fragment of the wheat *Actin* gene (AB181991) or the Arabidopsis *Tubulin* gene (AT1G04820), with three independent replicates per experiment. The specificity of the real-time PCR was confirmed by agarose gel electrophoresis of the amplicon. The analysis was confirmed three times.

Chromosomal Location of *TaOPR1*

The chromosomal location of *TaOPR1* was obtained via a PCR strategy based on the amplification of genomic DNA extracted from a set of wheat cultivar Chinese Spring nullitetrasonic lines (Sears, 1954) and a partial set of

ditelocentric lines (Sears and Sears, 1978). Each 20- μ L PCR contained 1 \times EasyTaq buffer, 0.2 μ M deoxyribonucleotide triphosphates, 0.5 μ M *TaOPR1*-specific primers (Supplemental Table S1), 0.5 unit of Easy Taq, and 100 ng of DNA, and the amplification regime consisted of an initial denaturation of 94°C/5 min, followed by 35 cycles of 94°C/40 s, 60°C/40 s, and 72°C/50 s, ending with a final extension of 72°C/10 min. The resulting amplicons were separated by agarose electrophoresis.

Subcellular Localization of *TaOPR1*

The *TaOPR1* sequence, lacking its stop codon, was ligated into the *Xba*I and *Bam*HI cloning sites of the 326-GFP vector. Either this recombinant plasmid or the empty 326-GFP was transformed into *Arabidopsis* mesophyll protoplasts following the method described by Yoo et al. (2007). After a 16-h incubation at 22°C in the dark, GFP signal was detected by bright-field and fluorescence microscopy.

Physiological Characterization

Three-leaf-stage wheat seedling leaves harvested from plants raised in one-half-strength Hoagland liquid medium and whole 2-week-old *Arabidopsis* seedlings were analyzed for the activity of the ROS-scavenging enzymes superoxide dismutase, CAT, and POD, following Sequeira and Mineo (1966), and for MDA content as described by Heath and Packer (1968). The experiment was performed three times.

Measurement of ROS and JA Levels

ROS level was visualized by DAB staining according to Asselbergh et al. (2007). Briefly, 3-week-old *Arabidopsis* seedlings were placed under light conditions and floated in a solution of 1 mg mL⁻¹ DAB-HCl (pH 4) at 28°C for 8 h, and then chlorophyll was removed with 95% ethanol in a boiling bath. JA content was measured by liquid chromatography-tandem mass spectrometry (LC-MS/MS) as follows. A total of 1,000 mg of fresh 3-week-old *Arabidopsis* seedlings was frozen in liquid nitrogen and well ground with a small glass pestle in a 2-mL vial. Following the addition of 1,000 μ L of methanol, homogenates were well mixed in an ultrasonic bath and then kept at 4°C overnight. After being centrifuged at 15,000g for 10 min, the supernatant was collected and then vacuumed to dryness in a Jouan RCT60 concentrator. Dried extract was dissolved in 200 μ L of sodium phosphate solution (0.1 mol L⁻¹, pH 7.8) and later passed through a Sep-Pak C₁₈ cartridge (Waters). JA was eluted with 1,500 μ L of 50% methanol and vacuumed to dryness again, redissolved in 50 μ L of 20% acetonitrile, and injected (5 μ L) into a LC20AD-MS8030 LC-MS/MS system (Shimadzu); a BEH C₁₈ (100 \times 2.1 mm, 1.7 μ m) column (Waters) was used, column temperature was 30°C, the mobile phase comprised 55% acetonitrile and 45% water (v/v), and the flow rate was 0.30 mL min⁻¹. Mass spectrography was operated in the negative mode under the following conditions: ionization, electrospray; capillary voltage, 3.5 kV; collision energy, 15 eV; desolvation temperature, 250°C; mass-to-charge ratio, 209.1/59.

The accession number of *TaOPR1* in GenBank is JQ409278.

Supplemental Data

The following materials are available in the online version of this article.

Supplemental Figure S1. *opr1opr2* double RNAi knockdown mutation does not change the response of *Arabidopsis* to NaCl and H₂O₂.

Supplemental Figure S2. The transcription of a set of well-established abiotic stress-responsive genes, based on RT-PCR.

Supplemental Table S1. PCR primer sequences used for this research.

ACKNOWLEDGMENTS

We thank Dr. Neil C. Bruce at the University of York for kindly providing *Arabidopsis opr1opr2* RNAi knockdown seeds.

Received November 29, 2012; accepted January 12, 2013; published January 15, 2013.

LITERATURE CITED

- Abe H, Urao T, Ito T, Seki M, Shinozaki K, Yamaguchi-Shinozaki K** (2003) *Arabidopsis* AtMYC2 (bHLH) and AtMYB2 (MYB) function as transcriptional activators in abscisic acid signaling. *Plant Cell* **15**: 63–78
- Agrawal GK, Jwa NS, Shibato J, Han O, Iwahashi H, Rakwal R** (2003) Diverse environmental cues transiently regulate OsOPR1 of the “octadecanoid pathway” revealing its importance in rice defense/stress and development. *Biochem Biophys Res Commun* **310**: 1073–1082
- Asselbergh B, Curvers K, Franca SC, Audenaert K, Vuylsteke M, Van Breusegem F, Höfte M** (2007) Resistance to *Botrytis cinerea* in *sitens*, an abscisic acid-deficient tomato mutant, involves timely production of hydrogen peroxide and cell wall modifications in the epidermis. *Plant Physiol* **144**: 1863–1877
- Beynon ER, Symons ZC, Jackson RG, Lorenz A, Rylott EL, Bruce NC** (2009) The role of oxophytodienoate reductases in the detoxification of the explosive 2,4,6-trinitrotoluene by *Arabidopsis*. *Plant Physiol* **151**: 253–261
- Biesgen C, Weiler EW** (1999) Structure and regulation of OPR1 and OPR2, two closely related genes encoding 12-oxophytodienoic acid-10,11-reductases from *Arabidopsis thaliana*. *Planta* **208**: 155–165
- Clough SJ, Bent AF** (1998) Floral dip: a simplified method for *Agrobacterium*-mediated transformation of *Arabidopsis thaliana*. *Plant J* **16**: 735–743
- Delker C, Stenzel I, Hause B, Miersch O, Feussner I, Wasternack C** (2006) Jasmonate biosynthesis in *Arabidopsis thaliana*: enzymes, products, regulation. *Plant Biol (Stuttg)* **8**: 297–306
- Esterbauer H** (1993) Cytotoxicity and genotoxicity of lipid-oxidation products. *Am J Clin Nutr (Suppl)* **57**: 779S–785S, discussion 785S–786S
- Fitzpatrick TB, Amrhein N, Macheroux P** (2003) Characterization of YqjM, an Old Yellow Enzyme homolog from *Bacillus subtilis* involved in the oxidative stress response. *J Biol Chem* **278**: 19891–19897
- Fujita Y, Fujita M, Shinozaki K, Yamaguchi-Shinozaki K** (2011) ABA-mediated transcriptional regulation in response to osmotic stress in plants. *J Plant Res* **124**: 509–525
- Hayashi M, Aoki M, Kato A, Kondo M, Nishimura M** (1996) Transport of chimeric proteins that contain a carboxy-terminal targeting signal into plant microbodies. *Plant J* **10**: 225–234
- He Y, Fukushige H, Hildebrand DF, Gan S** (2002) Evidence supporting a role of jasmonic acid in *Arabidopsis* leaf senescence. *Plant Physiol* **128**: 876–884
- Heath RL, Packer L** (1968) Photoperoxidation in isolated chloroplasts. I. Kinetics and stoichiometry of fatty acid peroxidation. *Arch Biochem Biophys* **125**: 189–198
- Jakab G, Ton J, Flors V, Zimmerli L, Métraux J-P, Mauch-Mani B** (2005) Enhancing *Arabidopsis* salt and drought stress tolerance by chemical priming for its abscisic acid responses. *Plant Physiol* **139**: 267–274
- Katsir L, Schmillier AL, Staswick PE, He SY, Howe GA** (2008) COI1 is a critical component of a receptor for jasmonate and the bacterial virulence factor coronatine. *Proc Natl Acad Sci USA* **105**: 7100–7105
- Kazan K, Manners JM** (2011) JAZ repressors and the orchestration of phytohormone crosstalk. *Trends Plant Sci* **17**: 22–31
- Kramell R, Miersch O, Atzorn R, Parthier B, Wasternack C** (2000) Octadecanoid-derived alteration of gene expression and the “oxylipin signature” in stressed barley leaves: implications for different signaling pathways. *Plant Physiol* **123**: 177–188
- Kumar S, Tamura K, Nei M** (2004) MEGA3: integrated software for molecular evolutionary genetics analysis and sequence alignment. *Brief Bioinform* **5**: 150–163
- Larkin MA, Blackshields G, Brown NP, Chenna R, McGettigan PA, McWilliam H, Valentin F, Wallace IM, Wilm A, Lopez R, et al** (2007) Clustal W and Clustal X version 2.0. *Bioinformatics* **23**: 2947–2948
- Laudert D, Hennig P, Stelmach BA, Müller A, Andert L, Weiler EW** (1997) Analysis of 12-oxo-phytyldienoic acid enantiomers in biological samples by capillary gas chromatography-mass spectrometry using cyclodextrin stationary phases. *Anal Biochem* **246**: 211–217
- Lee SC, Luan S** (2012) ABA signal transduction at the crossroad of biotic and abiotic stress responses. *Plant Cell Environ* **35**: 53–60
- Liu C, Li S, Wang M, Xia GM** (2012) A transcriptomic analysis reveals the nature of salinity tolerance of a wheat introgression line. *Plant Mol Biol* **78**: 159–169
- Livak KJ, Schmittgen TD** (2001) Analysis of relative gene expression data using real-time quantitative PCR and the 2^{- $\Delta\Delta$ CT} method. *Methods* **25**: 402–408

- Miao Y, Lv D, Wang P, Wang XC, Chen J, Miao C, Song CP (2006) An *Arabidopsis* glutathione peroxidase functions as both a redox transducer and a scavenger in abscisic acid and drought stress responses. *Plant Cell* **18**: 2749–2766
- Miersch O, Wasternack C (2000) Octadecanoid and jasmonate signaling in tomato (*Lycopersicon esculentum* Mill.) leaves: endogenous jasmonates do not induce jasmonate biosynthesis. *Biol Chem* **381**: 715–722
- Mittler R (2002) Oxidative stress, antioxidants and stress tolerance. *Trends Plant Sci* **7**: 405–410
- Mittler R, Kim Y, Song L, Coutu J, Coutu A, Ciftci-Yilmaz S, Lee H, Stevenson B, Zhu JK (2006) Gain- and loss-of-function mutations in *Zat10* enhance the tolerance of plants to abiotic stress. *FEBS Lett* **580**: 6537–6542
- Mittler R, Vanderauwera S, Suzuki N, Miller G, Tognetti VB, Vandepoele K, Gollery M, Shulaev V, Van Breusegem F (2011) ROS signaling: the new wave? *Trends Plant Sci* **16**: 300–309
- Mueller MJ, Brodschelm W (1994) Quantification of jasmonic acid by capillary gas chromatography-negative chemical ionization-mass spectrometry. *Anal Biochem* **218**: 425–435
- Munns R, Tester M (2008) Mechanisms of salinity tolerance. *Annu Rev Plant Biol* **59**: 651–681
- Nakashima K, Ito Y, Yamaguchi-Shinozaki K (2009) Transcriptional regulatory networks in response to abiotic stresses in *Arabidopsis* and grasses. *Plant Physiol* **149**: 88–95
- Nankivell BJ, Chen J, Boadle RA, Harris DC (1994) The role of tubular iron accumulation in the remnant kidney. *J Am Soc Nephrol* **4**: 1598–1607
- Odat O, Matta S, Khalil H, Kampranis SC, Pfau R, Tschlis PN, Makris AM (2007) Old yellow enzymes, highly homologous FMN oxidoreductases with modulating roles in oxidative stress and programmed cell death in yeast. *J Biol Chem* **282**: 36010–36023
- Parchmann S, Gundlach H, Mueller MJ (1997) Induction of 12-oxo-phytodienoic acid in wounded plants and elicited plant cell cultures. *Plant Physiol* **115**: 1057–1064
- Peng Z, Wang M, Li F, Lv H, Li C, Xia G (2009) A proteomic study of the response to salinity and drought stress in an introgression strain of bread wheat. *Mol Cell Proteomics* **8**: 2676–2686
- Reymond P, Weber H, Damond M, Farmer EE (2000) Differential gene expression in response to mechanical wounding and insect feeding in *Arabidopsis*. *Plant Cell* **12**: 707–720
- Schaller F, Biesgen C, Müssig C, Altmann T, Weiler EW (2000) 12-Oxophytodienoate reductase 3 (OPR3) is the isoenzyme involved in jasmonate biosynthesis. *Planta* **210**: 979–984
- Schaller F, Hennig P, Weiler EW (1998) 12-Oxophytodienoate-10,11-reductase: occurrence of two isoenzymes of different specificity against stereoisomers of 12-oxophytodienoic acid. *Plant Physiol* **118**: 1345–1351
- Schaller F, Weiler EW (1997) Molecular cloning and characterization of 12-oxophytodienoate reductase, an enzyme of the octadecanoid signaling pathway from *Arabidopsis thaliana*: structural and functional relationship to yeast old yellow enzyme. *J Biol Chem* **272**: 28066–28072
- Sears ER (1954) The aneuploids of common wheat. *Mo Agric Exp Sta Res Bull* **572**: 1–58
- Sears ER, Sears LMS (1978) The Telocentric Chromosomes of Common Wheat. Indian Agricultural Research Institute, New Delhi, India
- Sequeira L, Mineo L (1966) Partial purification and kinetics of indoleacetic acid oxidase from tobacco roots. *Plant Physiol* **41**: 1200–1208
- Stelmach BA, Müller A, Hennig P, Laudert D, Andert L, Weiler EW (1998) Quantitation of the octadecanoid 12-oxo-phytodienoic acid, a signalling compound in plant mechanotransduction. *Phytochemistry* **47**: 539–546
- Stenzel I, Hause B, Maucher H, Pitzschke A, Miersch O, Ziegler J, Ryan CA, Wasternack C (2003) Allene oxide cyclase dependence of the wound response and vascular bundle-specific generation of jasmonates in tomato: amplification in wound signalling. *Plant J* **33**: 577–589
- Stintzi A, Browse J (2000) The *Arabidopsis* male-sterile mutant, *opr3*, lacks the 12-oxophytodienoic acid reductase required for jasmonate synthesis. *Proc Natl Acad Sci USA* **97**: 10625–10630
- Strassner J, Fürholz A, Macheroux P, Amrhein N, Schaller A (1999) A homolog of old yellow enzyme in tomato: spectral properties and substrate specificity of the recombinant protein. *J Biol Chem* **274**: 35067–35073
- Strassner J, Schaller F, Frick UB, Howe GA, Weiler EW, Amrhein N, Macheroux P, Schaller A (2002) Characterization and cDNA-microarray expression analysis of 12-oxophytodienoate reductases reveals differential roles for octadecanoid biosynthesis in the local versus the systemic wound response. *Plant J* **32**: 585–601
- Trotter EW, Collinson EJ, Dawes IW, Grant CM (2006) Old yellow enzymes protect against acrolein toxicity in the yeast *Saccharomyces cerevisiae*. *Appl Environ Microbiol* **72**: 4885–4892
- Wang MC, Peng ZY, Li CL, Li F, Liu C, Xia GM (2008) Proteomic analysis on a high salt tolerance introgression strain of *Triticum aestivum*/*Thinopyrum ponticum*. *Proteomics* **8**: 1470–1489
- Weber H, Vick BA, Farmer EE (1997) Dinor-oxo-phytodienoic acid: a new hexadecanoid signal in the jasmonate family. *Proc Natl Acad Sci USA* **94**: 10473–10478
- Weiler EW, Kutchan TM, Gorba T, Brodschelm W, Niesel U, Bublitz F (1994) The *Pseudomonas* phytotoxin coronatine mimics octadecanoid signalling molecules of higher plants. *FEBS Lett* **345**: 9–13
- Williams RE, Bruce NC (2002) “New uses for an old enzyme”: the Old Yellow Enzyme family of flavoenzymes. *Microbiology* **148**: 1607–1614
- Xia GM (2009) Progress of chromosome engineering mediated by asymmetric somatic hybridization. *J Genet Genomics* **36**: 547–556
- Xia GM, Xiang FN, Zhou AF, Wang H, Chen HM (2003) Asymmetric somatic hybridization between wheat (*Triticum aestivum* L.) and *Agropyron elongatum* (Host) Nevishi. *Theor Appl Genet* **107**: 299–305
- Yan J, Zhang C, Gu M, Bai Z, Zhang W, Qi T, Cheng Z, Peng W, Luo H, Nan F, et al (2009) The *Arabidopsis* CORONATINE INSENSITIVE1 protein is a jasmonate receptor. *Plant Cell* **21**: 2220–2236
- Yoo S-D, Cho Y-H, Sheen J (2007) *Arabidopsis* mesophyll protoplasts: a versatile cell system for transient gene expression analysis. *Nat Protoc* **2**: 1565–1572
- Zhao TJ, Zhao SY, Chen HM, Zhao QZ, Hu ZM, Hou BK, Xia GM (2006) Transgenic wheat progeny resistant to powdery mildew generated by *Agrobacterium* inoculum to the basal portion of wheat seedling. *Plant Cell Rep* **25**: 1199–1204
- Ziegler J, Keinänen M, Baldwin IT (2001) Herbivore-induced allene oxide synthase transcripts and jasmonic acid in *Nicotiana attenuata*. *Phytochemistry* **58**: 729–738